Expression of a replication-dependent core histone in post-mitotic neurons

Yuichi Uosaki[a], Kenji Ito[b], Azumi Noguchi[a], Hirokazu Arakawa[c], Takumi Takizawa[a]*

[a] Department of Pediatrics, Graduate School of Medicine, Gunma University, 3-39-22 Showa-machi, Maebashi, Gunma 371-8511, Japan

[b] Division of Stem Cell Pathology, Center for Experimental Medicine and Systems Biology, Institute of Medical Science, Tokyo University, Minato-ku, Tokyo108-8639, Japan

[c] Kitakanto Allergy institute, Midori-shi, Gunma, Japan

* **Correspondence**:

Takumi Takizawa

takizawt@gunma-u.ac.jp

Abstract

Neurons express numerous genes in response to environmental stimuli. This activity-dependent transcription is vital for neurons to function and, hence, for the brain to perform its complex processes. Post-translational modifications of core histones have been implicated in the regulation of neuronal activity-dependent transcription. Moreover, transcription and repair also involve the exchange of core histones, which regulates histone metabolism; however, its involvement in neural activity-dependent transcription remains unknown. Here, in mature postmitotic neurons derived from the mouse hippocampus, the *Hist1h3f* gene, which encodes replication-dependent histone H3.2, is expressed upon stimulation of glutamine receptors. Salt extraction and metabolic labeling of newly synthesized proteins in neurons revealed that core histone proteins are increased in terms of their protein levels in response to glutamine receptor stimulation. These results suggest that newly synthesized replication-dependent histones play a role in post-mitotic neurons.

Keywords: Histone variant H3.2, Chromatin, Nucleosome, Neuron, Neuronal activity, Transcription

Abbreviations

Aha, azidohomoalanine; CaMK, calmodulin-dependent protein kinase; CREB, cAMP

response element binding protein; Daxx, death domain associated protein 6; GABA, gamma amino butyric acid; HIRA, histone cell cycle regulator A; MNase, micrococcal nuclease.

Introduction

Numerous genes are actively transcribed in response to external stimuli in neurons, forming the molecular basis of neuroplasticity. Neuroplasticity is a functional feature of the brain that alters its responsiveness in response to external stimuli (Greer and Greenberg, 2008; Hardingham et al., 2018; Yap and Greenberg, 2018), alongside increasing the binding surface and number of dendritic spines and promoting protein synthesis in the formation of long-term memory (Borrelli et al., 2008; Chen et al., 2017; Hamilton et al., 2012; West and Greenberg, 2011). Upon stimulation of glutamate receptors at the postsynaptic sites, intracellular calcium levels increase (Malgaroli and Tsien 1992), leading to calmodulin-dependent protein kinase (CaMK) II/IV activation (Impey et al., 2002) and the consequent activation of cAMP response element binding protein (CREB) (Kornhauser et al., 2002) and others (Yap and Greenberg, 2018). CREB activates the transcription of its target genes with CREB-binding protein, a histone acetyl transferase (Bading, 2013; Bito et al., 1996; West and Greenberg, 2011).

A nucleosome consists of 147 bp of DNA and an octamer of two sets of four types of

core histones, H2A, H2B, H3, and H4. Each of the four types of core histones forms a family, and more than 100 histone genes are found in the mammalian genome (Marzluff et al., 2002). There are various types of variants in histones (Martire and Banaszynski, 2020; Talbert et al., 2012). H3 variants include replication-dependent histones H3.1 and H3.2 and replication-independent histone H3.3 (Henikoff and Smith, 2015). Replication-dependent histones are used to build chromatin on the nascent strand during S-phase in a DNA synthesis-dependent manner, while replication-independent histones are incorporated at any stage of the cell cycle (Ray-Gallet et al., 2002; Tagami et al., 2004). Although the amino acid sequences of H3.1 and H3.3 differ only in five residues, their functions are different; H3.3 is more frequently found and turnover in enhancer and regulatory regions of actively transcribed genes than H3.1 and H3.2. This suggests that the nucleosomes containing H3.3 are more unstable than those containing H3.1 or H3.2 (Deaton et al., 2016; Harada et al., 2012). Several factors, such as histone post-translational modification (Tropberger et al., 2013), chromatin remodelers (Kobor et al., 2004), and histone chaperones (Goldberg et al., 2010), affect the stability of the nucleosome and hence influence the process of histone exchange or turnover.

In post-mitotic neurons, transcription is active, meaning histone post-translational modifications are highly dynamic (Brami-Cherrier et al., 2006). DNA methylation is also

highly variable; some genomic regions are repeatedly methylated and demethylated in response to neural activity, which is enabled by the exchange of nucleic acids (Ma et al., 2009). It has been suggested that the exchange or turnover of histone variants is important for neural activity-dependent gene expression in nervous system cells (Michod et al., 2012; Santoro and Dulac, 2012; Zovkic et al., 2014). For example, H3.3 increases with age in mammalian neurons, in contrast to a marked decrease in H3.1 and H3.2 (Maze et al., 2015; Piña and Suau, 1987). In this study, we report the active transcription of genes encoding histone H3.2 in post-mitotic neurons. The results indicate that the nature of histone turnover is different in the early stages of neuronal development from that in the late stages.

Materials and Methods

Cell culture and stimulation of hippocampal neurons

All animal experimental procedures were approved by the Animal Care and Experimentation Committee of Gunma University. Hippocampal neurons from ICR mice at embryonic day (E) 17.5 were cultured as previously described (Kaech and Banker, 2006) with modifications. Briefly, timed pregnant ICR mice (Japan SLC, City, Country)

were killed by cervical dislocation. Hippocampi were carefully dissected from embryos and washed once in Hanks' balanced salt solution (HBSS) and were then digested with 3 mL of papain solution containing 1500 units of DNase I (Sigma-Aldrich, D4527), 1 mg of L-cysteine, 25 mg of D (+)-Glucose, 1 mg of bovine serum albumin (BSA) (Invitrogen, 15260), and 100 µL of papain (Sigma-Aldrich P3125) for 20 min at 37 °C in a water bath. The hippocampi were suspended in HBSS with 1 mL of DNase solution containing 500 units of DNase I and 3 mg of magnesium sulfate heptahydrate. It was then triturated with fire-polished Pasteur pipettes and passed through a 70-µm cell strainer (BD-Falcon 352340) to remove debris. After centrifugation (1050 rpm, 4 °C, 8 min) of the cells in PBS with 7.5% BSA, the cells were suspended in alpha-MEM (Invitrogen 11095–080) and plated onto poly-L-lysine-coated 10-cm plastic dishes at a density of 1.7 million cells per dish. After 4 h, the medium was replaced with Neurobasal medium (Thermo Fisher 21103-149) with MACS NeuroBrew-21 (Millteny Biotech 130-093-566) and the cells were further cultured under 5% O_2 conditions (Wright and Shay, 2006). To inhibit the proliferation of astrocytes and other proliferating cells on days *in vitro* 4 (DIV 4), 10 µM cytosine β-D-arabinofuranoside (Sigma-Aldrich C1768) was added to the culture media. Neurons were depolarized by activation of sub-synaptic glutamate receptors with 50 µM bicuculline and 2.5 mM 4-aminopyridine (4-AP), a weak potassium ion (K^+) channel

blocker (Hardingham et al., 2001). When used, cycloheximide, a protein synthesis inhibitor, was added to the medium at a final concentration of 100 μM.

Microarrays

Cells were collected at 0, 30, 180, and 300 min after bicuculline and 4-AP stimulation. Total RNA was extracted using the RNAeasy kit (Qiagen). RNAs were labeled and hybridized on the Mouse Gene ST1.0 array (Affymetrix). Two biological replicates were analyzed for each time point. Intensity values after hybridization were normalized to the median intensity of the chip, and ratios of the expression levels of 30, 180, and 300 min to the 0 min time point were calculated for each gene. Genes showing at least 1.5-fold differences at 30 and 180 min are shown in Supplemental Table 1.

RNA isolation and quantitative reverse transcription (RTq)-PCR

Total RNA was extracted with the ToTALLY RNA total RNA isolation kit (Thermo Fisher) and then treated with DNase I. Complementary DNA was generated by reverse transcription using oligo (dT) primer (Thermo Fisher, 18418012) or random primers (Thermo Fisher, 48190011), and SuperScript II Reverse Transcriptase (Thermo Fisher, 18064022) according to the manufacturer's instructions. Quantitative real-time PCR

(qPCR) was performed using the KAPA STBR Fast qPCR Kit (Kapa Biosystems) using LightCycler 480 (Roche). Gene expression was normalized to glyceraldehyde-3-phosphate dehydrogenase (*Gapdh)* mRNA levels. The following primers were used: 5'-TTGGAAACAAGGCTTTCAG-3' and 5'-CCCAAACTGAAGTGCGTACC-3' (*Hist1h3f*), 5'-AGAACATCATCCCTGCATCC-3' and 5'-CACATTGGGGGTAGGAACAC-3' (*Gapdh*).

Protein extraction from salt-treated nuclei

Hippocampal cultured neurons were washed once with ice-cold PBS, scraped off, and collected in falcon tubes. Cells were resuspended in 600 μL buffer A (15 mM Tris-HCl pH 8, 15 mM NaCl, 60 mM KCl, 1mM EDTA pH 8, 0.5 mM EGTA, and 0.5 mM spermidine) with protease inhibitor (Nacalai Tesque 25955–11) after centrifugation at 8000 × g for 10 min at 4 °C, and the cell suspension was incubated in an equivalent amount of buffer A added with 0.2% NP-40 (Wako 599–05781) on ice for 10 min occasionally mixed gently upside-down. After centrifugation at 500 × g for 10 min at 4 °C, cell pellets were treated with 100 mM NaCl and rotated at 4 °C for 1 h. Supernatants were incubated at 95 °C for 5 min with 6 × sodium dodecyl sulfate (SDS) sample buffer, 7 mL of 0.5 M Tris-HCl pH 6.8, 1 g SDS, 3 mL of glycerol, 1.2 mg bromophenol blue, and 10

μM dithiothreitol (DTT) after centrifugation at 15000 × g for 10 min at 4 °C and stored at −30 °C. The insoluble fraction was stored with SDS sample buffer as described above.

Western blot

Western blotting was performed using Trans-Blot Turbo Systems (Bio-Rad) with 4% gradient gels. Membranes were probed with anti-H3 (Abcam ab1791), streptavidin (stAv)-HRP (GE Healthcare RPN 1231V), or anti-H3.3 (Rat moAb 0.23 mg/mL, a kind gift from Professor Yasuyuki Ohkawa, Department of Advanced Medical Initiatives, JST-CREST, Faculty of Medicine, Kyusyu University, Fukuoka, Japan). Signals were detected with horseradish peroxidase (HRP)-conjugated anti-rabbit (GE Healthcare NA934V), HRP-conjugated anti-mouse (GE Healthcare NA93), and HRP-conjugated anti-rat (GE Healthcare NA935V) using an ECL prime kit (GE Healthcare RPN2132).

Non-radioactive labeling of newly synthesized proteins

Labeling of newly synthesized proteins was carried out as previously described (Deal et al., 2010) with a slight modification. In brief, on DIV 10, neurons were washed twice with methionine (Met)-free DMEM (Gibco 21013–024) and incubated at 37 °C for 30 to 60 min in Met-free medium. After replacing the medium with Met-free DMEM again, 4

mM azidohomoalanine (Aha; Anaspec 63669), a methionine analogue, was added to the culture medium, and the cells were further incubated for 3 h. The cells were collected, washed once in ice-cold PBS, and suspended in buffer A with a 1% protease inhibitor cocktail. An equal volume of buffer A with 0.2% NP-40 was added and placed on ice for 10 min. The cell suspension was incubated on ice for 10 min with occasional stirring. After centrifugation (500 × g, 4 °C, 10 min), the supernatant was discarded and nuclei pellets were washed in buffer A and then centrifuged again. The nuclei were resuspended in HB125 buffer (0.125 M Sucrose, 15 mM Tris-HCl [pH 7.5], 15 mM NaCl, 40 mM KCl, 0.5 mM spermidine, and 0.15 mM spermine), and Aha-incorporated proteins were labeled with biotin by incubation at 4 °C overnight in the presence of 0.5 mM biotin-alkyne (Invitrogen B10185), 1 mM $CuSO_4$, and 50 mM ascorbic acid. Biotin-labeled cell nuclei were resuspended in MNase buffer (10 mM Tris-HCl [pH7.4], 15 mM NaCl, 60 mM KCl, 0.15 mM spermine, 0.5 mM spermidine with 2000 gel unit MNase [New England Biolabs M0247]) and incubated for 1 h at 25 °C. MNase reactions were quenched by adding 2 mM EDTA and pelleting nuclei by centrifugation at 500 × g for 10 min at 4 °C. Nuclei were resuspended in 300 μL CSB 350 buffer (1 × PBS, 350 mM NaCl, 2 mM EDTA, 0.1% Triton X-100) and rotated at 4 °C for 16 h. The soluble chromatin was centrifuged at 4 °C for 5 min at 13000 × g. The supernatants were incubated at 55 °C for 2 h to

denature the non-nucleosomal proteins (Tachiwana et al., 2010). After centrifugation (10,000 × g, 4 °C, 5 min), the supernatant was collected. For the input, one-fifth of the volume of the supernatant was used. M280 Streptavidin-Dynabeads (Invitrogen 112.05D) was added to the remaining supernatant and rotated at 4 °C for at least 1.5 h. stAv-beads were collected on a magnet rack, and beads were resuspended in Urea wash buffer (4 M Urea, 0.3 M NaCl, 20 mM Tris-HCl [pH 8]) for 5 min at 4 °C to remove other histone H2A/ H2B or DNA binding proteins (Yamasu', 1990). Beads were collected as described above and prepared for western blotting.

RI in situ hybridization

The DNA template (plasmid DNA; pGEMT-easy vector and inserted DNA) was amplified by PCR. The PCR reaction was performed as follows: 94 °C, 5 min, (94 °C, 1 min + 53 °C, 1 min + 72 °C, 4 min) × 30 cycles, 72 °C, 7 min, 10 °C, hold. The PCR products were electrophoresed, and the gels were purified using GENECLEAN Kit (Q-Bio gene 1001–200) and phenol extraction. The PCR fragments were stored at −30 °C. S^{35-} riboprobes were prepared as previously described (Chen et al., 2012; Horita et al., 2012, 2010). The PCR DNA (0.2–0.3 μg/μL) fragment was incubated with 2 μL of 5 × optimized transcription buffer (Promega), 100 mM DTT, 0.3 μL of RNasin (Promega

N251B), 1.5 μL of 10 mM of each AGC mix, 10 μL of 100 mM ATP (Roche 1140965) + 90 μL of pure water, 10 μL of 100 mM GTP (Roche 1140957) + 90 μL pure water, 10 μL of 100 mM CTP (Roche 1140922) + 90 μL of pure water, 4.5 μL of S35-UTP (PerkinElmer NEG-039H), and 1 μL of RNA polymerase (Promega) for 2 h at 37 °C. Next, up to 50 μL with 40 μL of pure water was added, and the solution was further incubated with 2.5 μL of 5 M NaCl and 125 μL of 100% EtOH at –80 °C for at least 15 min. After centrifugation at 15,000 rpm at 4 °C for more than 15 min, the supernatant was rinsed with 70% EtOH and centrifuged again. The precipitate was dissolved with 10 μL of pure water and incubated at 65 °C for 5 min, then immediately chilled on ice. For each probe, the probe was mixed with 40 μL of hybridization solution (5 mL of 100% formamide, 600 μL of 5 M NaCl, 100 μL of 1 M Tris-HCl [pH 8], 240 μL of 0.5 M EDTA [pH 8], 200 μL of 50 × Denhart's solution, 100 μL of 1 M DTT, 250 μL of 20 mg/mL tRNA [Roche 109495], 1 g SDS). Next, the tubes were incubated at 65 °C in water baths for 5 min and immediately chilled on ice. The slides were covered and placed in small plastic racks at 65 °C. The slides were hybridized at room temperature for 12–15 h. Subsequent washing steps were performed as follows. The slides were washed twice with chloroform and then placed into 2 × SSPE; 3 M NaCl, 0.2 M NaH_2PO_4 ・H_2O (pH 7.4)) + 0.1% β-mercaptoethanol solution. The glass slides were rinsed in 2 × SSPE + 0.1% β-

mercaptoethanol solution immediately and incubated in 2 × SSPE + 0.1% β-mercaptoethanol solution for 30 min at room temperature, with gently swinging. The slides were incubated at 65 °C in a pre-warmed 50% formamide, 2 × SSPE, and 0.1% β-mercaptoethanol solution for 1 h, with occasional gentle swinging. The slides were incubated twice in pre-warmed 50% formamide, 2× SSPE, and 0.1% β-mercaptoethanol solution for 30 min, occasionally gently swinging. Finally, the sections were dried in 50%, 70%, 95%, and 100% EtOH for 2 min and then exposed to X-ray film (Bio-Max MR Kodak, Rochester, NY).

Animal treatment and behavioral experiments

For *in situ* hybridization, the control brain was assessed over the course of an 8–10 h photoperiod. Metrazol (GABAa receptor antagonist) was administered at 15 mg/mL for 1 h, confirming the induction of an epileptic condition. Forced running mice were housed with running wheels (Fast-Trac, BioServ K3250) and forced to run for 1 h. For voluntary running, C57/BL6 male mice at postnatal day 28 were individually housed in plastic cages with free access to water and pellet diet according to a 12 h light and dark cycle. The mice were housed with running wheels and allowed to run freely in their cage for approximately 2 months.

Results

Activity-dependent expression of H3.2 genes in hippocampal neurons

We assessed the activity-dependent transcription in hippocampal neurons in a genome-wide manner using a microarray. We found that *Hist1h3f*, which encodes a replication-dependent core histone, H3.2, was increased in depolarized neurons (Figure 1A). Because replication-dependent histones are synthesized during the S-phase to rapidly package the newly replicated genome DNA as chromatin in proliferating cells, we further investigated this unexpected induction of H3.2 expression in post-mitotic neurons. We next performed RT-qPCR to confirm the microarray results. Histone H3.2 is encoded by nine genes that house only one similar exon each in mice (Pandey et al., 1990) (Figure 1B), all of which do not undergo poly-A tail modification, but instead have a conserved stem-loop structure (Marzluff et al., 2008). Among the nine genes, *Hist1h3f* and *Hist1h3e* share unique longer 3' UTR sequences (Figure 1B). We designed primer pairs for this shared 3' UTR. With these primers, *Hist1h3f* and *Hist1h3e* are distinguished from other H3.2 genes, but not from each other. The expression of *Hist1h3f* and *Hist1h3e* mRNA gradually increased in response to bicuculline and 4-AP -induced depolarization (Figure 1C). It is worth noting that reverse transcription with oligo (dT) primers also resulted in an increase. This indicated that *Hist1h3f* and *Hist1h3e* had a poly A tail in post-mitotic neurons. These

results indicate that histone genes encoding H3.2 are expressed in post-mitotic neurons in an activity-dependent manner.

Figure 1

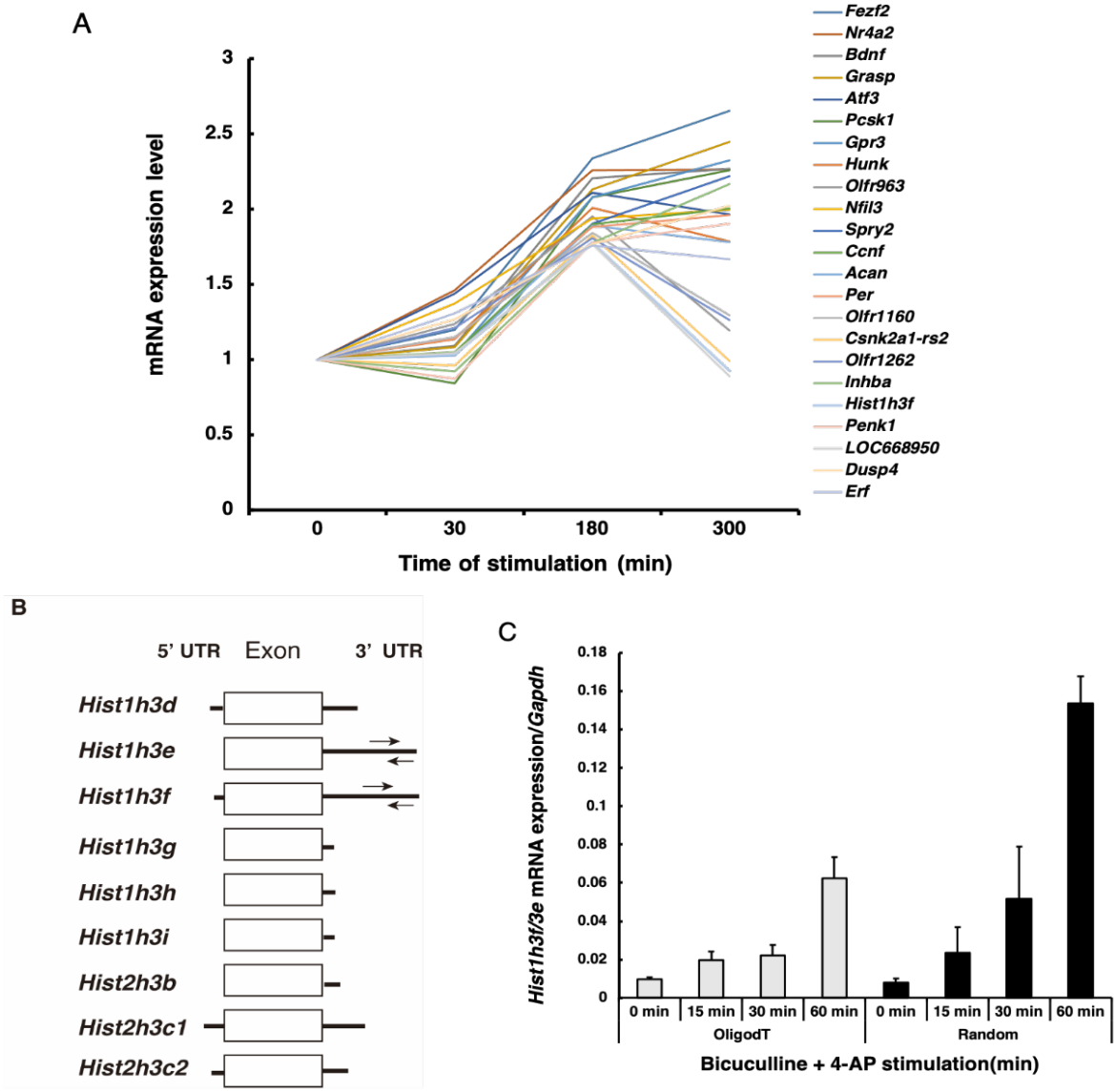

Figure 1. mRNA expression of *Hist1h3f* and *Hist1h3e in vitro*. **(A)** Activity-dependent mRNAs expression analysis with microarray at 10 days *in vitro* (DIV) primary cultured hippocampal neurons. These genes' expression levels increased over 1.5 times in 180 min after depolarization. The level of *Hist1h3f*, one of the replication-dependent histone genes in mice, was increased. **(B)** Genes that encode H3.2 mRNA in mouse. Arrows point to primers designed at the unique 3' UTR region of *Hist1h3f* and *Hist1h3e*. **(C)** qRT-PCR of *Hist1h3f* and *Hist1h3e* mRNA. RNA molecules were collected from hippocampal neurons cultured for 10 days *in vitro* after being treated with 50 μM bicuculline and 200 μM 4-aminopyridine (4-AP) at different time points, and reverse transcribed with either oligo(dT) or random hexamer primers to synthesize cDNA. The expression levels of *Hist1h3f* and *Hist1h3e* mRNA were normalized to *Gapdh*.

H3.2 expression in the adult mouse brain

We next assessed the expression of *Hist1h3f* and *Hist1h3e* in the brain. Expression patterns of *Hist1h3f* or *Hist1h3e* mRNA were detected in the hippocampus, cerebellum, and olfactory bulb in the adult brain by *in situ* hybridization (Figure 2A). Cells that express the genes included neurons, as assessed based on expression patterns across brain regions. Expression was also assessed in a gray matter, representing expression patterns

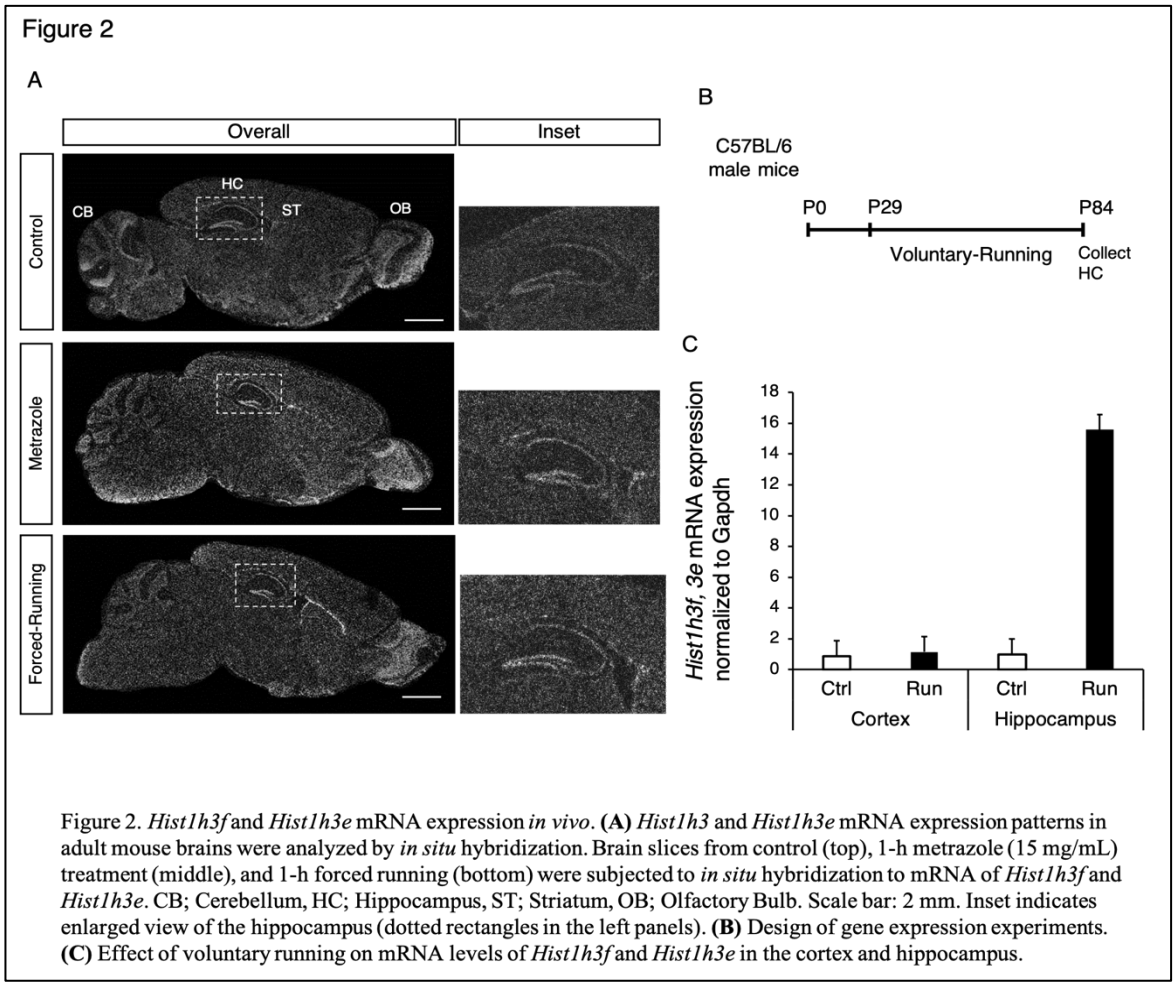

Figure 2. *Hist1h3f* and *Hist1h3e* mRNA expression *in vivo*. **(A)** *Hist1h3* and *Hist1h3e* mRNA expression patterns in adult mouse brains were analyzed by *in situ* hybridization. Brain slices from control (top), 1-h metrazole (15 mg/mL) treatment (middle), and 1-h forced running (bottom) were subjected to *in situ* hybridization to mRNA of *Hist1h3f* and *Hist1h3e*. CB; Cerebellum, HC; Hippocampus, ST; Striatum, OB; Olfactory Bulb. Scale bar: 2 mm. Inset indicates enlarged view of the hippocampus (dotted rectangles in the left panels). **(B)** Design of gene expression experiments. **(C)** Effect of voluntary running on mRNA levels of *Hist1h3f* and *Hist1h3e* in the cortex and hippocampus.

in other types of cells. The expression of *Hist1h3f* or *Hist1h3e* mRNA was observed in

normal conditions, the levels of which remained constant or slightly increased either after a GABAa receptor antagonist treatment, which induced convulsions, or after 1 hour of forced running (Figure 2A). We next quantitated *Hist1h3f* or *Hist1h3e* mRNA expression in the adult brain by RT-qPCR. The mRNA expression was detected both in the cortex and hippocampus and increased after housing mice in a voluntary running condition for 2 months (Figure 2B, 2C).

Increase in H3 expression after depolarization

We examined whether H3 is increased at the protein level in hippocampal neurons. Because the amino acid sequences of H3.1 and H3.2 differ only by one residue, there is no antibody that selectively recognizes H3.2, but not H3.1. Therefore, we used an antibody that recognizes pan-H3 proteins. Initially, we assessed an increase in the total amount of histone H3 in whole nuclear lysates, but were unable to detect an increase due to the large quantity of existing histones that were incorporated into the chromatin. Therefore, we next quantified levels of histone H3 that were not incorporated into or loosely bound to chromatin using a salt extraction technique that extracts proteins that are loosely bound to chromatin (Meshorer et al., 2006). In the supernatant from cell nuclei after treatment with a 100 mM NaCl solution, H3 was increased in neurons

simultaneously stimulated with bicuculline and 4-AP (Figure 3A). The increase disappeared by inhibiting protein synthesis with cycloheximide. These results indicated that the increase was due to protein synthesis rather than the release of existing H3 from chromatin (Figure 3B). The H3.3 variant was not detected in the same salt-extracted

Figure 3

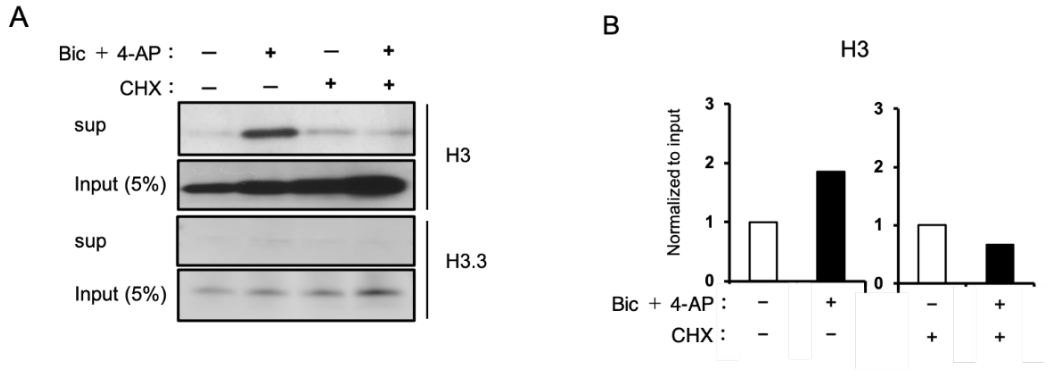

Figure 3. H3 proteins in salt-extracted supernatants. **(A)** Western blot analysis with antibodies against total H3 (upper two rows) and H3.3 (bottom two rows). Nuclei were isolated from depolarized hippocampal neurons, and re-suspended in 100 mM NaCl, and incubated at 4 ˚C for 1 h with rotating. The supernatants (sup) and whole nuclear lysates (input) were subjected to western blotting. Cycloheximide (CHX, 100 μg/mL) was added for 20 min. **(B)** Quantification of H3

fraction, indicating that H3.3 was not synthesized under these conditions.

Metabolic labeling of newly synthesized proteins

To directly determine whether H3 is translated in an activity-dependent manner, we next

performed metabolic labeling of newly synthesized proteins in neurons using Aha (Figure 4A). The smear band was detected both in the bicuculine- and 4-AP-treated or untreated

Figure 4

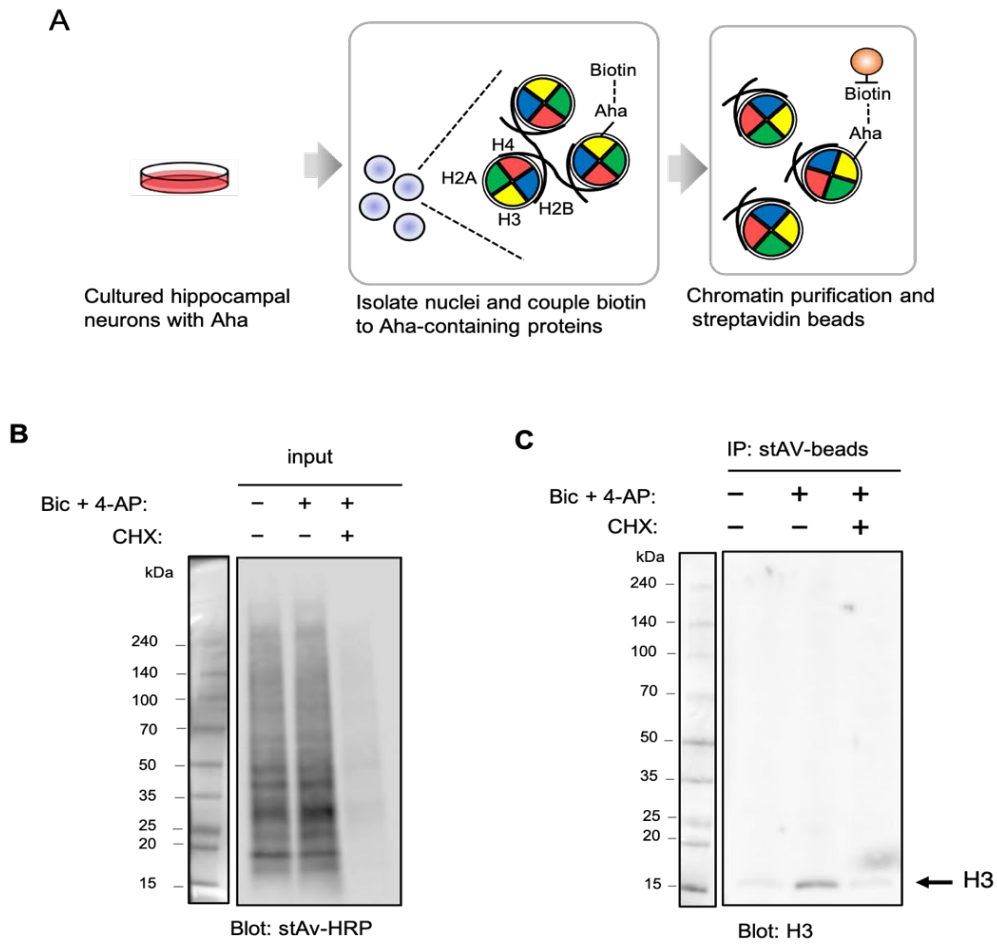

Figure 4. Metabolic labelling of newly synthesized protein in neurons. **(A)** Schematic depiction of the labeling of newly synthesized proteins in primary hippocampal neurons. **(B)** Chromatin fractions prepared from nuclei after metabolic labelling were electrophoresed and blotted with streptavidin (stAv)-HRP. **(C)** Biotin-labelled proteins were immunoprecipitated (IP) with streptavidin-beads and subjected to western blotting. Antibody against pan-H3 antibody was used. Bic; bicuculline, 4-AP; 4-aminopyridine, CHX; Cycloheximide.

neurons and was hardly detected in cycloheximide-pretreated neurons, indicating that the newly synthesized proteins were effectively labeled (Figure 4B). We next enriched the

chromatin fraction after MNase treatment after metabolic labeling and collected newly synthesized biotinylated proteins with stAv-beads. Next, precipitates were subjected to western blotting with an antibody against histone H3 (Figure 4C). H3 was readily detected in polarized neurons compared to non-polarized neurons or CHX-treated neurons. The results suggested that H3 was synthesized and possibly partially incorporated into chromatin in a neural activity-dependent manner (Figure 4C).

Discussion

We demonstrated that the levels of *Hist1h3f* and *Hist1h3e*, which encode a replication-dependent core histone, H3.2, were increased in mouse hippocampal neurons in an activity-dependent manner. Using salt extraction and metabolic labeling, we also found that the replication-dependent core histone H3 was increased at protein levels in an activity-dependent manner in post-mitotic neurons.

In proliferating cells, the transcription of replication-dependent histones is restricted to the S-phase and its products lack a poly A tail (Dominski and Marzluff, 1999). Lyons et al. reported that a subset of replication-dependent histone mRNAs are polyadenylated in terminally differentiated tissues (Lyons et al., 2016). Our results indicated that *Hist1h3f* and *Hist1h3e* cDNAs were detected after reverse transcription

with oligo dT primers, indicating that at least some fractions of mRNAs of these genes were polyadenylated in terminally differentiated post-mitotic neurons.

Many neuronal activity-dependent genes are transcribed through CREB activation (Hardingham et al., 2001; Hong et al., 2008; Kornhauser et al., 2002). Indeed, there exists a CRE, a CREB-binding sequence, on the promoter region of the *Hist1h3f* gene, which might be relevant to its activity-dependent transcription.

Hist1h3f and *Hist1h3e* were expressed in the adult mouse hippocampus. Their expression was rather constant under convulsive conditions or forced running. This appeared inconsistent with the results obtained for primary cultured neurons. One possible explanation for this is the difference in developmental stages between brain slices and cultured neurons. It is difficult to pinpoint which developmental stage cultured neurons belong to; however, these were prepared from embryos. The cells are postmitotic and, while considered morphologically mature, may still be in the early developmental stages. We speculated that *Hist1h3f* and *Hist1h3e* are expressed robustly in an activity-dependent manner in the early stages, while they are expressed more statically in the later stages.

Indeed, it has been shown that protein levels of H3.1 and H3.2 decreased with aging in the rodent brain, whereas H3.3 levels increased with an inverse relationship to age

(Maze et al., 2015; Piña and Suau, 1987; Tvardovskiy et al., 2017). Remarkably, H3.3 was incorporated into the gene body of transcriptionally active genes in post-mitotic neurons, and its load increases with aging. In addition, the knockdown of genes that encode H3.3 in mouse neurons causes cognitive and learning deficits (Maze et al., 2015). This suggests that the expression of histone variant H3.3 and its replacement with existing replication-dependent core histones may be associated with functional changes in neurons underlying neuronal plasticity. Our current finding demonstrating the expression of H3.2 at early developmental stages indicates that H3.2 may have a similar role in developing neurons.

Histone chaperones such as Daxx (Michod et al., 2012) and HIRA (Maze et al., 2015) have been shown to play a role in H3.3 incorporation into chromatin in a neural activity-dependent manner. However, the histone chaperone that regulates the incorporation of H3.2 into chromatin has not been identified so far (Hammond et al., 2017). Shedding light on H3.2 incorporation into chromatin and its underlying mechanisms in the future will be of great interest in terms of H3 metabolism in neurons and, thus, in brain neuroplasticity specifically during development.

Funding

This work was supported by JSPS KAKENHI Grant Number JP 23650167.

CRediT authorship contribution statement

Yuichi Uosaki: Data curation; Formal analysis; Validation; Visualization

Writing - original draft; **Takumi Takizawa:** Conceptualization; Funding acquisition; Methodology; Project administration; Resources; Supervision; Visualization; Writing-original draft; Writing - review & editing. **Kenji Ito and Azumi Noguchi:** data acquisition and critical discussion**. Hirokazu Arakawa**: critical discussion, supervision experiments.

Declaration of interest

There are no conflicts of interest to declare.

Acknowledgments

We thank all members of the Department of Pediatrics for their critical help and advice. Anti-H4K5ac (mouse 2 mg/mL) and anti-H3.3 (Rat moAb 0.23 mg/mL) were kindly provided by Professor Hiroshi Kimura (Cell Biology center, Institute of Innovative Research, Tokyo Institute of Technology, Yokohama, Japan) and Dr. Ohkawa

(Department of Advanced Medical Initiatives, JST-CREST, Faculty of Medicine, Kyusyu University, Fukuoka, Japan), respectively.

References

Bading, H., 2013. Nuclear calcium signalling in the regulation of brain function. Nat Rev Neurosci 14, 593–608. https://doi.org/10.1038/nrn3531

Bito, H., Deisseroth, K., Tsien, R.W., 1996. CREB Phosphorylation and Dephosphorylation: A Ca2+- and Stimulus Duration–Dependent Switch for Hippocampal Gene Expression. Cell 87, 1203–1214. https://doi.org/10.1016/S0092-8674(00)81816-4

Borrelli, E., Nestler, E.J., Allis, C.D., Sassone-Corsi, P., 2008. Decoding the Epigenetic Language of Neuronal Plasticity. Neuron 60, 961–974. https://doi.org/10.1016/j.neuron.2008.10.012

Brami-Cherrier, K., Lavaur, J., Pagès, C., Arthur, J.S.C., Caboche, J., 2006. Glutamate induces histone H3 phosphorylation but not acetylation in striatal neurons: role of mitogen- and stress-activated kinase-1: MSK1 and nucleosomal response in neurons. Journal of Neurochemistry 101, 697–708. https://doi.org/10.1111/j.1471-4159.2006.04352.x

Chen, C.-C., Wada, K., Jarvis, E.D., 2012. Radioactive in situ Hybridization for Detecting Diverse Gene Expression Patterns in Tissue. JoVE 3764. https://doi.org/10.3791/3764

Chen, L.-F., Zhou, A.S., West, A.E., 2017. Transcribing the connectome: roles for transcription factors and chromatin regulators in activity-dependent synapse development. Journal of Neurophysiology 118, 755–770. https://doi.org/10.1152/jn.00067.2017

Deal, R.B., Henikoff, J.G., Henikoff, S., 2010. Genome-Wide Kinetics of Nucleosome Turnover Determined by Metabolic Labeling of Histones. Science 328, 1161–1164. https://doi.org/10.1126/science.1186777

Deaton, A.M., Gómez-Rodríguez, M., Mieczkowski, J., Tolstorukov, M.Y., Kundu, S., Sadreyev, R.I., Jansen, L.E., Kingston, R.E., 2016. Enhancer regions show high histone H3.3 turnover that changes during differentiation. eLife 5, e15316. https://doi.org/10.7554/eLife.15316

Dominski, Z., Marzluff, W.F., 1999. Formation of the 3′ end of histone mRNA. Gene 239, 1–14. https://doi.org/10.1016/S0378-1119(99)00367-4

Goldberg, A.D., Banaszynski, L.A., Noh, K.-M., Lewis, P.W., Elsaesser, S.J., Stadler, S., Dewell, S., Law, M., Guo, X., Li, X., Wen, D., Chapgier, A., DeKelver, R.C., Miller, J.C., Lee, Y.-L., Boydston, E.A., Holmes, M.C., Gregory, P.D., Greally, J.M., Rafii, S., Yang, C., Scambler, P.J., Garrick, D., Gibbons, R.J., Higgs, D.R., Cristea, I.M., Urnov, F.D., Zheng, D., Allis, C.D., 2010. Distinct Factors Control Histone Variant H3.3 Localization at Specific Genomic Regions. Cell 140, 678–691. https://doi.org/10.1016/j.cell.2010.01.003

Greer, P.L., Greenberg, M.E., 2008. From Synapse to Nucleus: Calcium-Dependent Gene Transcription in the Control of Synapse Development and Function. Neuron 59, 846–860. https://doi.org/10.1016/j.neuron.2008.09.002

Hamilton, A.M., Oh, W.C., Vega-Ramirez, H., Stein, I.S., Hell, J.W., Patrick, G.N., Zito, K., 2012. Activity-Dependent Growth of New Dendritic Spines Is Regulated by the Proteasome. Neuron 74, 1023–1030. https://doi.org/10.1016/j.neuron.2012.04.031

Hammond, C.M., Strømme, C.B., Huang, H., Patel, D.J., Groth, A., 2017. Histone chaperone networks shaping chromatin function. Nat Rev Mol Cell Biol 18, 141–158. https://doi.org/10.1038/nrm.2016.159

Harada, A., Okada, S., Konno, D., Odawara, J., Yoshimi, T., Yoshimura, S., Kumamaru, H., Saiwai, H., Tsubota, T., Kurumizaka, H., Akashi, K., Tachibana, T., Imbalzano, A.N., Ohkawa, Y., 2012. Chd2 interacts with H3.3 to determine myogenic cell fate: Chd2 incorporates H3.3 to mark myogenic genes. The EMBO Journal 31, 2994–3007. https://doi.org/10.1038/emboj.2012.136

Hardingham, G.E., Arnold, F.J.L., Bading, H., 2001. Nuclear calcium signaling controls CREB-mediated gene expression triggered by synaptic activity. Nat Neurosci 4, 261–267. https://doi.org/10.1038/85109

Hardingham, G.E., Pruunsild, P., Greenberg, M.E., Bading, H., 2018. Lineage divergence of activity-driven transcription and evolution of cognitive ability. Nat Rev Neurosci 19, 9–15. https://doi.org/10.1038/nrn.2017.138

Henikoff, S., Smith, M.M., 2015. Histone Variants and Epigenetics. Cold Spring Harb Perspect Biol 7, a019364. https://doi.org/10.1101/cshperspect.a019364

Hong, E.J., McCord, A.E., Greenberg, M.E., 2008. A Biological Function for the Neuronal Activity-Dependent Component of Bdnf Transcription in the Development of Cortical Inhibition. Neuron 60, 610–624. https://doi.org/10.1016/j.neuron.2008.09.024

Horita, H., Kobayashi, M., Liu, W., Oka, K., Jarvis, E.D., Wada, K., 2012.

Specialized Motor-Driven dusp1 Expression in the Song Systems of Multiple Lineages of Vocal Learning Birds. PLoS ONE 7, e42173. https://doi.org/10.1371/journal.pone.0042173

Horita, H., Wada, K., Rivas, M., Hara, E., Jarvis, E.D., 2010. The dusp1 immediate early gene is regulated by natural stimuli predominantly in sensory input neurons. J. Comp. Neurol. NA-NA. https://doi.org/10.1002/cne.22370

Impey, S., Fong, A.L., Wang, Y., Cardinaux, J.-R., Fass, D.M., Obrietan, K., Wayman, G.A., Storm, D.R., Soderling, T.R., Goodman, R.H., 2002. Phosphorylation of CBP Mediates Transcriptional Activation by Neural Activity and CaM Kinase IV. Neuron 34, 235–244. https://doi.org/10.1016/S0896-6273(02)00654-2

Kaech, S., Banker, G., 2006. Culturing hippocampal neurons. Nat Protoc 1, 2406–2415. https://doi.org/10.1038/nprot.2006.356

Kobor et al_2004_A Protein Complex Containing the Conserved Swi2-Snf2-Related ATPase Swr1p.pdf, n.d.

Kornhauser, J.M., Cowan, C.W., Shaywitz, A.J., Dolmetsch, R.E., Griffith, E.C., Hu, L.S., Haddad, C., Xia, Z., Greenberg, M.E., 2002. CREB Transcriptional Activity in Neurons Is Regulated by Multiple, Calcium-Specific Phosphorylation Events. Neuron 34, 221–233. https://doi.org/10.1016/S0896-6273(02)00655-4

Lyons, S.M., Cunningham, C.H., Welch, J.D., Groh, B., Guo, A.Y., Wei, B., Whitfield, M.L., Xiong, Y., Marzluff, W.F., 2016. A subset of replication-dependent histone mRNAs are expressed as polyadenylated RNAs in terminally differentiated tissues. Nucleic Acids Res gkw620. https://doi.org/10.1093/nar/gkw620

Ma et al_2009_Neuronal Activity-Induced Gadd45b Promotes Epigenetic DNA Demethylation and.pdf, n.d.

Malgaroli 1992 -Glutamate-induced long-term potentiation of the frequency of miniature synaptic currents in cultured hippocampal neurons, n.d.

Martire, S., Banaszynski, L.A., 2020. The roles of histone variants in fine-tuning chromatin organization and function. Nat Rev Mol Cell Biol 21, 522–541. https://doi.org/10.1038/s41580-020-0262-8

Marzluff, W.F., Gongidi, P., Woods, K.R., Jin, J., Maltais, L.J., 2002. The Human and Mouse Replication-Dependent Histone Genes. Genomics 80, 487–498. https://doi.org/10.1006/geno.2002.6850

Marzluff, W.F., Wagner, E.J., Duronio, R.J., 2008. Metabolism and regulation

of canonical histone mRNAs: life without a poly(A) tail. Nat Rev Genet 9, 843–854. https://doi.org/10.1038/nrg2438

Maze, I., Wenderski, W., Noh, K.-M., Bagot, R.C., Tzavaras, N., Purushothaman, I., Elsässer, S.J., Guo, Y., Ionete, C., Hurd, Y.L., Tamminga, C.A., Halene, T., Farrelly, L., Soshnev, A.A., Wen, D., Rafii, S., Birtwistle, M.R., Akbarian, S., Buchholz, B.A., Blitzer, R.D., Nestler, E.J., Yuan, Z.-F., Garcia, B.A., Shen, L., Molina, H., Allis, C.D., 2015. Critical Role of Histone Turnover in Neuronal Transcription and Plasticity. Neuron 87, 77–94. https://doi.org/10.1016/j.neuron.2015.06.014

Meshorer, E., Yellajoshula, D., George, E., Scambler, P.J., Brown, D.T., Misteli, T., 2006. Hyperdynamic Plasticity of Chromatin Proteins in Pluripotent Embryonic Stem Cells. Developmental Cell 10, 105–116. https://doi.org/10.1016/j.devcel.2005.10.017

Michod, D., Bartesaghi, S., Khelifi, A., Bellodi, C., Berliocchi, L., Nicotera, P., Salomoni, P., 2012. Calcium-Dependent Dephosphorylation of the Histone Chaperone DAXX Regulates H3.3 Loading and Transcription upon Neuronal Activation. Neuron 74, 122–135. https://doi.org/10.1016/j.neuron.2012.02.021

Pandey, N.B., Chodchoy, N., Liu, T.-J., Marzluff, W.F., 1990. Introns in histone genes alter the distribution of 3′ ends. Nucl Acids Res 18, 3161–3170. https://doi.org/10.1093/nar/18.11.3161

Piña, B., Suau, P., 1987. Changes in histones H2A and H3 variant composition in differentiating and mature rat brain cortical neurons. Developmental Biology 123, 51–58. https://doi.org/10.1016/0012-1606(87)90426-X

Ray-Gallet, D., Quivy, J.-P., Scamps, C., Martini, E.M.-D., Lipinski, M., Almouzni, G., 2002. HIRA Is Critical for a Nucleosome Assembly Pathway Independent of DNA Synthesis. Molecular Cell 9, 1091–1100. https://doi.org/10.1016/S1097-2765(02)00526-9

Santoro, S.W., Dulac, C., 2012. The activity-dependent histone variant H2BE modulates the life span of olfactory neurons. eLife 1, e00070. https://doi.org/10.7554/eLife.00070

Tachiwana, H., Kagawa, W., Osakabe, A., Kawaguchi, K., Shiga, T., Hayashi-Takanaka, Y., Kimura, H., Kurumizaka, H., 2010. Structural basis of instability of the nucleosome containing a testis-specific histone variant, human H3T. Proceedings of the National Academy of Sciences 107, 10454–10459. https://doi.org/10.1073/pnas.1003064107

Tagami, H., Ray-Gallet, D., Almouzni, G., Nakatani, Y., 2004. Histone H3.1

and H3.3 Complexes Mediate Nucleosome Assembly Pathways Dependent or Independent of DNA Synthesis. Cell 116, 51–61. https://doi.org/10.1016/S0092-8674(03)01064-X

Talbert, P.B., Ahmad, K., Almouzni, G., Ausió, J., Berger, F., Bhalla, P.L., Bonner, W.M., Cande, W., Chadwick, B.P., Chan, S.W.L., Cross, G.A.M., Cui, L., Dimitrov, S.I., Doenecke, D., Eirin-López, J.M., Gorovsky, M.A., Hake, S.B., Hamkalo, B.A., Holec, S., Jacobsen, S.E., Kamieniarz, K., Khochbin, S., Ladurner, A.G., Landsman, D., Latham, J.A., Loppin, B., Malik, H.S., Marzluff, W.F., Pehrson, J.R., Postberg, J., Schneider, R., Singh, M.B., Smith, M., Thompson, E., Torres-Padilla, M.-E., Tremethick, D., Turner, B.M., Waterborg, J., Wollmann, H., Yelagandula, R., Zhu, B., Henikoff, S., 2012. A unified phylogeny-based nomenclature for histone variants. Epigenetics & Chromatin 5, 7. https://doi.org/10.1186/1756-8935-5-7

Tropberger, P., Pott, S., Keller, C., Kamieniarz-Gdula, K., Caron, M., Richter, F., Li, G., Mittler, G., Liu, E.T., Bühler, M., Margueron, R., Schneider, R., 2013. Regulation of Transcription through Acetylation of H3K122 on the Lateral Surface of the Histone Octamer. Cell 152, 859–872. https://doi.org/10.1016/j.cell.2013.01.032

Tvardovskiy, A., Schwämmle, V., Kempf, S.J., Rogowska-Wrzesinska, A., Jensen, O.N., 2017. Accumulation of histone variant H3.3 with age is associated with profound changes in the histone methylation landscape. Nucleic Acids Research 45, 9272–9289. https://doi.org/10.1093/nar/gkx696

West, A.E., Greenberg, M.E., 2011. Neuronal Activity-Regulated Gene Transcription in Synapse Development and Cognitive Function. Cold Spring Harbor Perspectives in Biology 3, a005744–a005744. https://doi.org/10.1101/cshperspect.a005744

Wright, W.E., Shay, J.W., 2006. Inexpensive low-oxygen incubators. Nat Protoc 1, 2088–2090. https://doi.org/10.1038/nprot.2006.374

Yamasu', K., 1990. Units of H3 and H4 Histones. J. Biochem. 107, 6.

Yap, E.-L., Greenberg, M.E., 2018. Activity-Regulated Transcription: Bridging the Gap between Neural Activity and Behavior. Neuron 100, 330–348. https://doi.org/10.1016/j.neuron.2018.10.013

Zovkic, I.B., Paulukaitis, B.S., Day, J.J., Etikala, D.M., Sweatt, J.D., 2014. Histone H2A.Z subunit exchange controls consolidation of recent and remote memory. Nature 515, 582–586. https://doi.org/10.1038/nature13707

Figure captions

Figure 1. mRNA expression of *Hist1h3f* and *Hist1h3e in vitro*. **(A)** Activity-dependent mRNAs expression analysis with microarray at 10 days *in vitro* (DIV) primary cultured hippocampal neurons. These genes' expression levels increased over 1.5 times in 180 min after depolarization. The level of *Hist1h3f*, one of the replication-dependent histone genes in mice, was increased. **(B)** Genes that encode H3.2 mRNA in mouse. Arrows point to primers designed at the unique 3' UTR region of *Hist1h3f* and *Hist1h3e*. **(C)** qRT-PCR of *Hist1h3f* and *Hist1h3e* mRNA. RNA molecules were collected from hippocampal neurons cultured for 10 days *in vitro* after being treated with 50 μM bicuculline and 200 μM 4-aminopyridine (4-AP) at different time points, and reverse transcribed with either oligo(dT) or random hexamer primers to synthesize cDNA. The expression levels of *Hist1h3f* and *Hist1h3e* mRNA were normalized to *Gapdh.*

Figure 2. *Hist1h3f* and *Hist1h3e* mRNA expression *in vivo*. **(A)** *Hist1h3* and *Hist1h3e* mRNA expression patterns in adult mouse brains were analyzed by *in situ* hybridization. Brain slices from control (top), 1-h metrazole (15 mg/mL) treatment (middle), and 1-h forced running (bottom) were subjected to *in situ* hybridization to mRNA of *Hist1h3f* and *Hist1h3e*. CB; Cerebellum, HC; Hippocampus, ST; Striatum, OB; Olfactory Bulb. Scale

bar: 2 mm. Inset indicates enlarged view of the hippocampus (dotted rectangles in the left panels). **(B)** Design of gene expression experiments. **(C)** Effect of voluntary running on mRNA levels of *Hist1h3f* and *Hist1h3e* in the cortex and hippocampus.

Figure 3. H3 proteins in salt-extracted supernatants. **(A)** Western blot analysis with antibodies against total H3 (upper two rows) and H3.3 (bottom two rows). Nuclei were isolated from depolarized hippocampal neurons, and re-suspended in 100 mM NaCl, and incubated at 4 ˚C for 1 h with rotating. The supernatants (sup) and whole nuclear lysates (input) were subjected to western blotting. Cycloheximide (CHX, 100 μg/mL) was added for 20 min. **(B)** Quantification of H3.

Figure 4. Metabolic labelling of newly synthesized protein in neurons. **(A)** Schematic depiction of the labeling of newly synthesized proteins in primary hippocampal neurons. **(B)** Chromatin fractions prepared from nuclei after metabolic labelling were electrophoresed and blotted with streptavidin (stAv)-HRP. **(C)** Biotin-labelled proteins were immunoprecipitated (IP) with streptavidin-beads and subjected to western blotting. Antibody against pan-H3 antibody was used. Bic, bicuculline; 4-AP, 4-aminopyridine; CHX, Cycloheximide.